

*Carnegie Observatories Astrophysics Series, Vol. 1:
Coevolution of Black Holes and Galaxies, 2003
ed. L. C. Ho (Pasadena: Carnegie Observatories,
<http://www.ociw.edu/ociw/symposia/series/symposium1/proceedings.html>)*

What Drives the Central Velocity Dispersion in Nearby Early-Type Galaxies?

G. A. VERDOES KLEIJN¹, R. P. VAN DER MAREL, and J. NOEL-STORR^{2,3}
(1) ESO, (2) STScI, (3) Columbia University

Abstract

The majority of nearby early-type galaxies contains detectable amounts of emission-line gas at their centers. The emission-line ratios and gas kinematics potentially form a valuable diagnostic of the nuclear activity and gravitational potential well. The observed central gas velocity dispersion often exceeds the stellar velocity dispersion. This could be due to either the gravitational potential of a black hole or turbulent shocks in the gas. Here we try to discriminate between these two scenarios.

1.1 Introduction

Optical emission-line gas is detected in at least 50% of the centers of nearby early-type (E/S0) galaxies (e.g., Phillips et al. 1986; Goudfrooij et al. 1994; Macchetto et al. 1996; Ho et al. 1997). The gas velocity dispersion σ_{gas} (corrected for instrumental broadening) typically increases towards the nucleus, reaching values similar to the central σ_{star} as measured through 100s of pc scale sized apertures (e.g., Zeilinger et al., 1996). Closer to the nucleus, σ_{gas} often exceeds σ_{star} (e.g., Ferrarese et al. 1996; Macchetto et al., 1997; van der Marel & van den Bosch 1998; Cappellari et al. 2002; Verdoes Kleijn et al. 2002). Potential contributors to σ_{gas} are motions due to (i) a black hole (BH) gravitational potential or (ii) shocks/turbulence in the gas. In the former case, σ_{gas} could be caused by three dimensional motion of collisionless cloudlets of gas. More likely, the collisional gas is expected to have settled in a disk. In that case, σ_{gas} will be caused by differential rotation over the aperture. However, shocks and/or turbulence can contribute to σ_{gas} if there is a permanent input of kinetic energy (perhaps the active galactic nucleus) to sustain them. Thus, determining the driver of σ_{gas} has implications for measurements of the BH mass (M_{BH}) and the flow properties of potential BH accretion material. Here we present preliminary modeling of σ_{gas} and σ_{star} in the nuclei of 16 active and 4 quiescent early-type galaxies to constrain the relative importance of gravitation and shocks/turbulence.

1.2 Sample and Data

The galaxy sample consists of 16 active galaxies with radio-jets taken from the UGC FR I sample (see Noel-Storr et al., these proceedings, for selection criteria) and four relatively quiescent early-type galaxies (NGC 3078, NGC 4526, NGC 6861 and IC 1459) (Table 1). The four quiescent early-type galaxies were selected to have central dust and/or

Table 1.1. *Early-Type Galaxy Sample.*

Galaxy	Type	M_B	D (Mpc)	Galaxy	Type	M_B	D (Mpc)
(1)	(2)	(3)	(4)	(1)	(2)	(3)	(4)
NGC 315	E+:	-21.9	67.9	M87	E+0-1 pec	-21.4	15.4
NGC 383	SA0-:	-21.4	65.2	NGC 5127	E pec	-20.6	64.4
NGC 541	cD	-21.2	73.3	NGC 5490	E	-21.1	69.2
NGC 741	E0:	-21.9	70.2	NGC 7052	E	-19.9	55.4
3C 66B	E	-21.1	84.8	3C 449	S0-:	-19.6	68.3
NGC 2329	S0-:	-21.1	76.7	NGC 7626	E pec:	-21.1	46.6
3C 264	E	-21.0	84.4	NGC 3078	E2-3	-20.6	35.2
UGC 7115	E	-20.4	90.5	NGC 4526	SAB(s)0	-20.5	16.9
NGC 4335	E	-20.3	61.5	NGC 6861	SA(s)0-:	-20.2	28.1
M84	E1	-20.8	15.4	IC 1459	E3	-21.1	29.2

The galaxies are taken from the UGC FR I radio galaxy sample (Noel-Storr et al., these proceedings) except for NGC 3078, NGC4526, NGC 6861 and IC 1459.

Col.(2): Hubble classification from NED. Col.(3): Absolute blue magnitude from LEDA. Col.(4): Distances from Faber et al. (1989), Tonry et al. (2001), or, if not available, directly from recession velocity and $H_0 = 75 \text{ km s}^{-1} \text{ Mpc}^{-1}$. Col.(5): Galaxy is part of the UGC FR I sample (1) or not (0).

gas disks. Four of the 21 UGC FR I galaxies were not included here because either σ_{star} is not available or the location of the nucleus could not be determined reliably, mainly due to dust obscuration

HST/STIS (HST/FOS for IC 1459) emission-line spectra are available for the sample. They include the $\text{H}\alpha + [\text{NII}]$ and $[\text{SII}]6716,6731$ lines. A central σ_{gas} per galaxy is determined by fitting single Gaussians to each of the lines in $\text{H}\alpha + [\text{NII}]$ and $[\text{SII}]6716,6731$ at the nucleus. An analytic emission-line flux profile is determined by fitting a double exponential to the emission-line surface brightness measurements from the HST/STIS spectra and HST/WFPC2 emission-line images (where available). The central stellar dispersion σ_{star} for the sample galaxies was obtained from the LEDA catalog*.

1.3 Collisionless Gas Models

Can the gravitational potential of a BH mass induce gas motions which explain σ_{gas} ? Current observations are consistent (e.g., Kormendy & Gebhardt 2001, for a review) with most (and perhaps all) early-type galaxies containing a black hole with a mass related to σ_{star} , i.e., the ' $M_{\text{BH}} - \sigma_{\text{star}}$ ' relation (Gebhardt et al. 2000; Ferrarese & Merritt 2000). We compute the expected σ_{gas} for such a BH mass under idealized circumstances. We assume the gas is a collisionless isotropic spherical distribution of gas clouplets orbiting the BH. The predicted gas velocity dispersion $\sigma_{\text{gas}}(\text{sphere},1)$ takes into account aperture size, PSF and instrumental line width.

Fig. 1.1a shows that σ_{gas} typically exceeds $\sigma_{\text{gas}}(\text{sphere},1)$. However, the calculation ne-

* LEDA database can be found at <http://leda.univ-lyon1.fr>

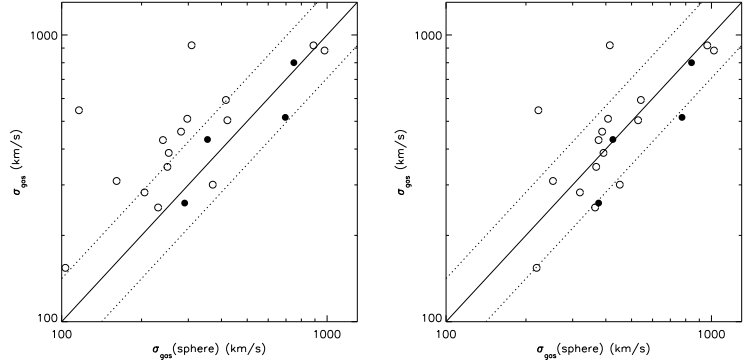


Fig. 1.1. The observed gas velocity dispersion σ_{gas} as a function of predicted velocity dispersions for radio galaxies (open circles) and relatively quiescent galaxies (filled circles). (a): The model for $\sigma_{\text{gas}}(\text{sphere},1)$ assumes an isotropic spherical distribution of gas cloudlets orbiting a BH with a mass according to the $M_{\text{BH}} - \sigma_{\text{star}}$ relation. (b): similar to (a) but now including the stellar mass distribution as well. The dashed and solid lines indicate $\sigma_{\text{gas}}(\text{sphere}) = (1/\sqrt{1/2}, 1, \sqrt{2}) \times \sigma_{\text{gas}}$ respectively (to facilitate comparison to the $M_{\text{BH}} - \sigma_{\text{star}}$). The figure suggests the gas might be largely collisionless: see text for details.

glects the stellar mass present, which will increase $\sigma_{\text{gas}}(\text{sphere},1)$. To illustrate the possible effect of this, Fig. 1.1b shows $\sigma_{\text{gas}}(\text{sphere},2)$ assuming an isothermal spherical stellar mass distribution in addition to the BH mass, i.e., $\sigma_{\text{gas}}^2(\text{sphere},2) = \sigma_{\text{gas}}^2(\text{sphere},1) + \sigma_{\text{star}}^2$. σ_{gas}^2 typically agrees within a factor 2 to $\sigma_{\text{gas}}^2(\text{sphere},2)$. In other words, the M_{BH} needed to account for σ_{gas}^2 agrees within a factor ~ 2 with M_{BH} as predicted by the $M_{\text{BH}} - \sigma_{\text{star}}$ relation (because $M_{\text{BH}} \sim \sigma_{\text{gas}}^2$), under these simplifying assumptions. The estimated intrinsic scatter in the relation is also a factor 2 (Tremaine et al. 2002). Thus, an additional contribution to σ_{gas} from collisions (e.g., shocks/turbulence) is not required in this case.

Alternatively, we can assume that the collisional gas settles in a disk. We idealize the disk as an infinitely flat disk of gas particles/cloudlets, inclined by 60° to the line of sight, and in circular rotation in the same combined BH and stellar potential as used in the spherical case. On the nucleus, the differential rotation will broaden the emission-line flux profile. Fig. 1.2a shows that the predicted gas velocity dispersion $\sigma_{\text{gas}}(\text{disk})$ roughly agrees with σ_{gas} . Hence no shocks/turbulence are required on average; a similar result as for the gas spherical model.

Gas dynamical models of galactic nuclei, based on gas mean velocity v_{gas} instead of σ_{gas} often reach a different conclusion. For five sample galaxies, the central BH mass has been measured directly from gas mean velocities v_{gas} in extended gas disks. Fig. 1.2b shows that the velocity dispersion $\sigma_{\text{gas}}(v_{\text{gas}})$ predicted by our gas disk model for *these* BH masses underpredicts σ_{gas} in four cases. Hence, an additional contributor to the velocity dispersion is needed to explain the observed values in our gas disk model. This agrees with the mean velocity modeling which invokes an additional source of dispersion, 'gas turbulence', to explain σ_{gas} (Maciejewski & Binney 2001; van der Marel & van den Bosch 1998; Cappellari et al. 2002; Verdoes Kleijn et al. 2002). Only for NGC 4486 does a detailed gas disk modeling by Macchetto et al. (1997) account for both v_{gas} and σ_{gas} , consistent with our

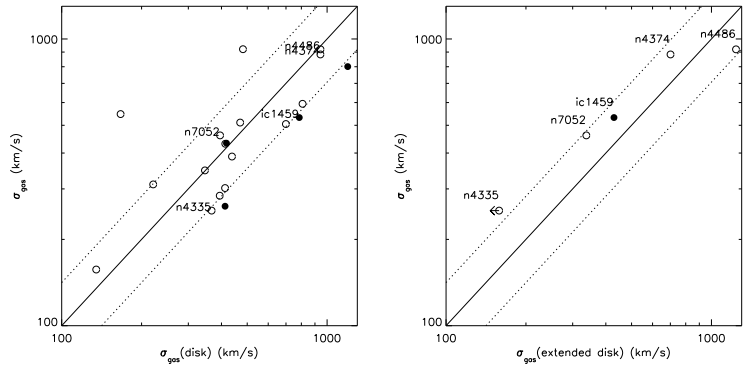


Fig. 1.2. The observed gas velocity dispersion σ_{gas} as a function of predicted velocity dispersions for radio galaxies (open circles) and relatively quiescent galaxies (filled circles). (a): The model assumes an infinitely thin gas disk in circular rotation, inclined by 60° to the line of sight and a BH mass M_{BH} according to the $M_{\text{BH}} - \sigma_{\text{star}}$ relation. (b): same as (a), but now for M_{BH} inferred from published, detailed modeling of the gas mean velocities v_{gas} . The figure suggests that v_{gas} and σ_{gas} cannot be simultaneously fit by the gas disk model: see text for further details.

modeling. It is reassuring that our simplistic modeling is consistent with the more detailed gas dynamical models on the difference between NGC 4486 and the other four galaxies.

It is less reassuring that Fig. 1.2b suggests that a thin, circular gas disk model in general cannot explain simultaneously observed gas velocities and dispersions. For a simultaneous fit one has to invoke gas turbulence. Alternatively, the extended gas might somehow rotate at subcircular velocities, which would lead the models to infer a lower BH mass and hence lower nuclear differential rotation.

Qualitatively, Fig. 1.1 suggests another possible solution to this problem: the gas changes from a flat disk configuration outside the nucleus to a (more) spherical distribution closer to the nucleus. The nuclear spherical gas distribution explains the central σ_{gas} . Furthermore, the new configuration implies that (i) the flat gas disk effectively has an inner radius and (ii) only part of the observed nuclear emission-line flux is coming from a disk. Both changes put the gas associated with the circular disk at a larger mean distance from the BH, compared to the continuous disk model, and hence at lower circular velocities for the same BH mass.

1.4 Discussion & Conclusions

The simple models discussed above suggest that the observed excess in velocity dispersion in nuclear emission-line gas disks could be explained by a more spherical gas distribution towards the nucleus. In such a model, the gas remains collisionless (as in the customary single gas disk model) and thus avoids invoking ad hoc turbulence or shocks which require a permanent input of kinetic energy to persist. Nevertheless, it could well be that activity associated with the BH can provide such a continuous input of energy. The outliers in Figs. 1.1 & 1.2 and the tendency for the collisionless models to underpredict σ_{gas} more for active galaxies rather than for quiescent galaxies perhaps favor this scenario.

More sophisticated modeling and further observations can help to determine between

different gas configurations. On the one hand, more accurate modeling of the stellar mass density and the emission-line velocity profiles are expected to decrease the predicted σ_{gas} at fixed BH mass. The central density profile of bright ellipticals is generally shallower than an isothermal distribution. Emission-lines often show extended wings: the true 2nd moment is then larger than the Gaussian 2nd moment. This effect is taken into account in the gas disk model, but not in the spherical model. On the other hand, emission-line flux profiles are typically marginally resolved. They may contain a significant contribution from an unresolved component which can be arbitrarily close to the BH. This might increase the predicted σ_{gas} .

UV spectroscopy can determine directly if shocks are present. In the presence of shocks the gas can be shock-ionized. If absent, the emission-line gas is only photo-ionized. The two ionization mechanisms produce different UV emission-line ratios (e.g., Dopita et al. 1997).

In summary, the current results cannot distinguish between the various gas configurations. However, accurate BH mass measurements (and hence BH demography) and BH accretion models depend on such a distinction. Improvement of the simplistic gas dynamical modeling presented here and UV observations can help to resolve this.

References

Cappellari, M., Verolme, E. K., van der Marel, R. P., Verdoes Kleijn, G. A., Illingworth, G. D., Franx, M., Carollo, C. M., & de Zeeuw, P. T. 2002, *ApJ*, 578, 787

Dopita, M. A., Koratkar, A. P., Allen, M. G., Tsvetanov, Z. I., Ford, H. C., Bicknell, G. V., & Sutherland, R. S. 1997, *ApJ*, 490, 202

Faber, S. M., Wegner, G., Burstein, D., Davies, R. L., Dressler, A., Lynden-Bell, D., & Terlevich, R. J. 1989, *ApJS*, 69, 763

Ferrarese, L., Ford, H. C., & Jaffe, W. 1996, *ApJ*, 470, 444

Ferrarese, L., & Merritt, D. 2000, *ApJ*, 539, L9

Gebhardt, K., et al. 2000, *ApJ*, 539, L13

Goudfrooij, P., Hansen, L., Jorgensen, H. E., & Norgaard-Nielsen, H. U. 1994, *A&AS*, 105, 341

Ho, L. C., Filippenko, A. V., & Sargent, W. L. W. 1997, *ApJ*, 487, 568

Kormendy, J., & Gebhardt, K. 2001, in The 20th Texas Symposium on Relativistic Astrophysics, ed. H. Martel & J. C. Wheeler (New York: AIP), 363

Macchetto, F. D., et al. 1996, *A&AS*, 120, 463

Macchetto, F. D., Marconi, A., Axon, D. J., Capetti, A., Sparks, W., & Crane, P. 1997, *ApJ* 489, 579

Maciejewski, W., & Binney, J. 2001, *MNRAS*, 323, 831

Phillips, M. M., Jenkins, C. R., Dopita, M. A., Sadler, E. M., & Binette, L. 1986, *AJ*, 91, 1062

Tonry, J., Dressler, A., Blakeslee, J. P., Ajhar, E. A., Fletcher, A. B., Luppino, G. A., Metzger, M. R., & Moore, C. B. 2001, *ApJ*, 546, 681

Tremaine, S., et al. 2002, *ApJ*, 574, 740

van der Marel, R. P., & van den Bosch, F. C. 1998, *AJ*, 116, 2220

Verdoes Kleijn, G. A., van der Marel, R. P., de Zeeuw, P. T., Noel-Storr, J., & Baum, S. A. 2002, *AJ*, 124, 2524

Zeilinger, W. W., et al. 1996, *A&AS*, 120, 257